

Transients of the Oxidation of Pyrimidines with $\text{SO}_4^{\bullet-}$: Structure and Reactivity of the Resulting Radicals

R. Lomoth, S. Naumov,[†] and O. Brede*

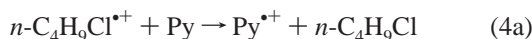
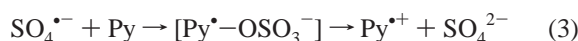
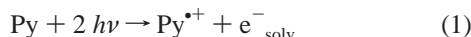
University of Leipzig, Interdisciplinary Group for Time-Resolved Spectroscopy, Permoserstr. 15, D-04303 Leipzig, Germany

Received: March 4, 1999; In Final Form: May 12, 1999

Depending on the methylation pattern, the reaction of $\text{SO}_4^{\bullet-}$ with various methylated pyrimidines yields radicals deprotonated at N(1) and C(5)–OH or C(6)–OH adduct radicals and probably allyl radicals by subsequent deprotonation at the C(5)-methyl group of the thymines. All of these radicals are derived from the initial $\text{SO}_4^{\bullet-}$ adducts on the pyrimidines that have lifetimes of several microseconds in the case of N(1)-methylated thymines. These transients could be taken for long-lived pyrimidine radical cations. However, spectral and kinetic comparison with the pyrimidine radical cations generated by electron transfer in nonpolar solvents (butyl chloride, acetone) reveals the adduct nature of these transients. In the course of sulfate adduct decay, pyrimidine radical cations could be formed as nondetectable short-lived ($\tau < 20\text{ns}$) intermediates rapidly reacting to the above-mentioned radical products. The reactivity of the $\text{SO}_4^{\bullet-}$ adducts, as well as that of the other pyrimidinyl radicals observed, was characterized by the subsequent oxidation of triphenylamine and di- or trimethoxybenzene, which supports the mechanistic interpretation given above. Hence there is no indication of long-lived pyrimidine radical cations under the conditions of the $\text{SO}_4^{\bullet-}$ oxidation of pyrimidines in aqueous solution.

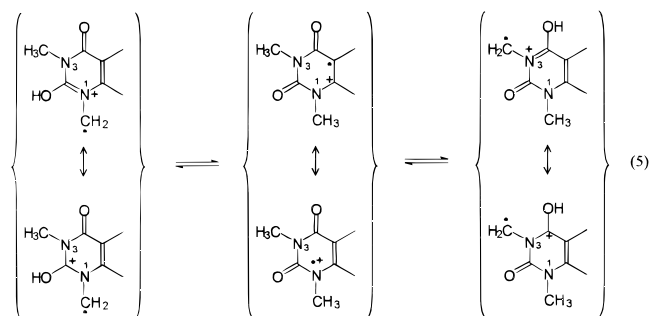
Introduction

Over the past few decades, the radiolysis of pyrimidines (Py) has been the subject of numerous studies^{1,2} as uracil, thymine, and cytosine are constituents of the nucleobase sequence of DNA and RNA. With regard to the direct effect of ionizing radiation, the radical cations of the nucleobases have attracted much attention because they give rise to the formation of base-OH radicals that have been shown to induce, with the intermediacy of sugar-centered radicals, strand breaks, and base release in nucleic acids.³ When modeling the processes occurring in the nucleic acids, useful methods for the ionization of the isolated pyrimidine bases were found to include direct photoionization⁴ by the absorption of two photons (1), triplet-sensitized electron transfer^{5,6} to excited carbonyl compounds (2), one-electron oxidation with radicals such as $\text{SO}_4^{\bullet-}$ ^{7–14} or $\text{Br}_2^{\bullet-}$ ^{15,16} (3), and electron transfer from radiation-generated parent radical cations^{17–19} in nonpolar solvents to the pyrimidines (Py) (4).



Despite taking place under conditions that are completely

different from biological conditions (*n*-butyl chloride or acetone as solvent), the latter method unequivocally generates pyrimidine radical cations which can be observed in the nanosecond time range with pulse radiolysis, as has recently been shown using the example of multiple methylated uracils and thymines.¹⁹ In that study, a transient tautomerism of $\text{Py}^{\bullet+}$ was found with the lactam form predominant in butyl chloride and the lactim form dominating in acetone (5).



The kinetic and spectroscopic properties of the pyrimidine radical cations available as found in ref 19 differ considerably from those of the species generated by the reaction of thymine derivatives with $\text{SO}_4^{\bullet-}$ (3) identified as radical cations by Deeble et al.,¹² who claimed to have direct evidence of pyrimidine radical cations surviving for a number of microseconds.

Comparing the optical absorption properties of the species formed in nonpolar (cf. reactions 4a,b) and aqueous solution (3), the maximum extinction coefficients in the visible range differ by a factor of between 3 and about 10 depending on the structure of $\text{Py}^{\bullet+}$ (lactam or lactim), as shown both in ref 19 and in this paper (Table 2). This fact casts doubt on whether

[†] Institute of Surface Modification, D-04303 Leipzig, Germany.

* Corresponding author.

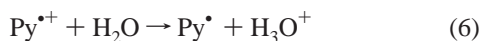
TABLE 1. Abbreviations and Sources of Supply of the Pyrimidine Derivatives Used

| | | |
|------------------------|-----------|-------------------|
| uracil | U | Aldrich, 98% |
| 1-methyluracil | 1-MU | Chemical Dynamics |
| 3-methyluracil | 3-MU | Fluka, >99% |
| 6-methyluracil | 6-MU | Sigma |
| 1,3-dimethyluracil | 1,3-DMU | Fluka, >99% |
| thymine | T | Aldrich, 99% |
| 1-methylthymine | 1-MT | Sigma |
| 3,6-Dimethylthymine | 3,6-DMT | <i>a</i> |
| 1,3-dimethylthymine | 1,3-DMT | <i>a</i> |
| 1,3,6-trimethylthymine | 1,3,6-TMT | <i>a</i> |

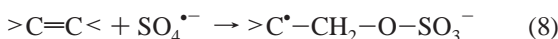
^a Derivative is not commercially available and was provided by S. Steenzen (Mülheim).

the species observed in water are indeed radical cations of the pyrimidines.

Characterizing pyrimidine radical cations in aqueous solution is impeded not only by deprotonation (low pK_a value of radical protonation (6)) and the nucleophilic addition of water (7) but also by the lack of information on the intermediate formation of metastable adducts of the oxidant radical to the unsaturated electron donor (3).



The sulfate radical is known to oxidize aromatic compounds directly in a one-electron-transfer process to radical cations,^{20–23} whereas reaction with olefins proceeds via more stable addition products.^{24,25} EPR studies by Davies and Gilbert²⁵ demonstrated that the reaction of alkenes and dienes with the sulfate radical anion (8) yields sulfate-substituted radicals that live for hundreds of microseconds.



Therefore, the primary reaction of $\text{SO}_4^{\bullet-}$ with the pyrimidines that are not aromatic²⁶ can be considered to be an addition to the olefinic double bond rather than one-electron oxidation. Hence, two extremes should be taken into account – very unstable sulfate adducts and the rapid formation of relatively stable $\text{Py}^{\bullet+}$ (variant of Deeble et al.¹²) or sulfate adducts as observable metastable intermediates, with $\text{Py}^{\bullet+}$ decaying immediately by the competition of (6) and (7) after its delayed formation due to (3), meaning $\text{Py}^{\bullet+}$ cannot be observed in aqueous solution.

To continue our studies into the properties of pyrimidine radical cations, in this paper we analyze the nature of the transients formed in aqueous solution by (i) comparing their optical properties with those obtained in nonpolar solution, (ii) analyzing their transient reaction dynamics, especially in respect of the subsequent oxidation of suitable reductants, and (iii) quantum-chemical considerations.

Experimental Section

The pyrimidines and their abbreviations are listed in Table 1. 1,4-dimethoxybenzene (Fluka, >99%) and 1,3,5-trimethoxybenzene (Fluka, >99%) were used without further purification. Triphenylamine (Laborchemie Apolda) was recrystallized twice from *n*-hexane. Solutions were prepared in water purified with a Millipore Milli-Q system and contained 0.01 M of potassium peroxodisulfate (Merck, >99%) and 0.5 M (2.5M for solubility reasons when using triphenylamine) of *tert*-butyl alcohol

(Merck, 99.8%). The standard pH of the solutions was 3.5 (H_2SO_4). Phosphate buffer (20mM) was used for pH variation experiments (pH 2–7). Buffer solutions were prepared from phosphorus pentoxide (Aldrich, 97%) and disodium hydrogen phosphate dihydrate (Merck, analytical grade). The pH of the solutions was measured before and after pulse radiolysis with a 540GLP pH meter (WTW). The solubility of triphenylamine and the methoxybenzenes in the water/*tert*-butyl alcohol mixtures was checked on a UV-2110PC photometer (Shimadzu). The solutions were deaerated by purging with nitrogen (99.999%).

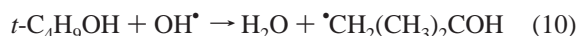
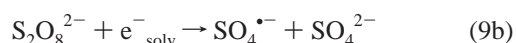
The samples were irradiated at room temperature with 15 ns, 20–100 Gy pulses of 1MeV electrons from an ELIT pulse transform accelerator (Institute of Nuclear Physics, Novosibirsk, Russia).

The optical detection system consisted of a pulsed XBO-900 xenon lamp (Osram), a SpectraPro-500 monochromator (Acton Research Corporation), an R4220 photomultiplier (Hamamatsu), and a TDS 640 digitizing oscilloscope (Tektronix).

Calculations were performed with HyperChem 5.01 using the semiempirical PM3 method²⁷ that has been applied with reasonable accuracy to open-shell systems. Geometries and spectra of the radicals calculated on the unrestricted Hartree–Fock (UHF) level did not differ markedly from those calculated with the restricted Hartree–Fock (RHF) approximation.

Results and Discussion

Reaction of Py with $\text{SO}_4^{\bullet-}$. Sulfate radical anions can be generated from peroxodisulfate by direct UV photolysis²⁸ or by reaction with solvated electrons²⁹ (9). The *G*-value for the formation of $\text{SO}_4^{\bullet-}$ amounts to 3.24 per 100 eV with a peroxodisulfate concentration of 10mM.³⁰ For rapid scavenging of OH radicals, *tert*-butyl alcohol was used in accordance with reaction 10.³¹ In the presence of 0.5M *tert*-butyl alcohol the sulfate radical anion decays with a lifetime of $\tau = 3 \mu\text{s}$ following a pseudo-first-order kinetics (i.e., nearly unaffected by the dose per pulse) due to the reaction with *tert*-butyl alcohol (inset Figure 1B).³² The rate constants of the reaction of the pyrimidines with the sulfate radical anion amount to $k_3 = (2–5) \times 10^9 \text{ M}^{-1} \text{ s}^{-1}$.^{8–12} Therefore, with a pyrimidine concentration of 5mM the sulfate radical anions can be considered to completely react (>97%) with the pyrimidines. (The yield decreases to 90% in the presence of 2.5M *tert*-butyl alcohol.)



The maximum extinction coefficients of the Py species observed were determined in two ways: (i) by transient concentration determination via electron dosimetry and (ii) using the absorption of the sulfate radical anion ($\lambda_{\text{max}} = 450 \text{ nm}$, $\epsilon_{450} = 1100 \text{ M}^{-1} \text{ cm}^{-1}$).³³

Spectra and assignment of $\text{SO}_4^{\bullet-}$ reaction products. The transient spectra obtained are given in Figure 1 for uracils and Figure 2 for thymine derivatives. Table 2 lists the optical extinction coefficients of the species obtained by the reaction of the pyrimidines with $\text{SO}_4^{\bullet-}$ together with literature data of the transients classified as radical cations by Deeble et al. (1-MT, 1,3-DMT, and 1,3,6-TMT)¹² and compares them with the extinction coefficients of the pyrimidine radical cations generated via free electron transfer in nonpolar media (reaction

TABLE 2. Absorption Maxima and Extinction Coefficients of Transients Obtained by Oxidation with $\text{SO}_4^{\bullet-}$ in Aqueous Solution and of Transients Resulting from Free Electron Transfer in Nonpolar Solvents (from Ref 19). Values in Parentheses from ref 12

| Py | butyl chloride | | acetone | | $\text{H}_2\text{O}/\text{SO}_4^{\bullet-}$ | | radical type |
|-----------|----------------------------------|---|----------------------------------|---|---|---|--------------|
| | $\lambda_{\text{max}}/\text{nm}$ | $\epsilon/\text{M}^{-1} \text{cm}^{-1}$ | $\lambda_{\text{max}}/\text{nm}$ | $\epsilon/\text{M}^{-1} \text{cm}^{-1}$ | $\lambda_{\text{max}}/\text{nm}$ | $\epsilon/\text{M}^{-1} \text{cm}^{-1}$ | |
| U | <i>a</i> | <i>a</i> | <i>a</i> | <i>a</i> | 410 550 | 830 660 | II |
| 1-MU | <i>a</i> | <i>a</i> | 380 570 | 3300 4100 | 400 | 940 | IIIa |
| 3-MU | <i>a</i> | <i>a</i> | 390 560 | 4300 ^b 4300 ^b | 410 570 | 980 640 | II |
| 6-MU | <i>a</i> | <i>a</i> | <i>a</i> | <i>a</i> | 450 550 | 1310 750 | II |
| 1,3-DMU | 400 | 13000 | 390 560 | 6600 6600 | 400 | 910 | IIIa |
| 1,3,6-TMU | 380 820 | 22000 11000 | 410 550 | 5700 6200 | | | |
| T | <i>a</i> | <i>a</i> | <i>a</i> | <i>a</i> | 400 500 | 1070 610 | II |
| 1-MT | <i>a</i> | <i>a</i> | 380 500 | 4300 3000 | 390 (400) | 1110 (1500) | I, IIIb |
| 1,3-DMT | 400 | 13000 | 380 520 | 5700 4000 | 400 (400) | 1250 (1660) | I |
| 3,6-DMT | <i>a</i> | <i>a</i> | 370 500 | 4500 3200 | 420 530 | 1180 520 | II |
| 1,3,6-TMT | 400 | 15000 | 400 500 | 5700 3600 | 410 (400) | 1360 (1480) | I |

^a No values due to insufficient solubility of Py. ^b Corrected values.

4a,b).¹⁹ The species obtained in water are evidently not identical with those produced in nonpolar media.

When assigning the spectra primarily observable after the reaction of the pyrimidines with $\text{SO}_4^{\bullet-}$, the following possibilities have to be considered:

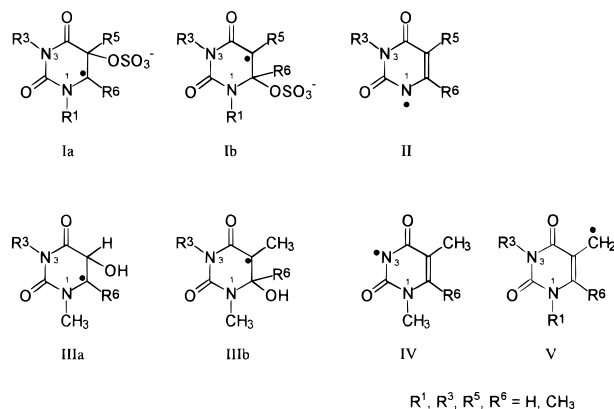
(i) The adduct (structure **I**) initially formed is a metastable but observable species. The electrophilic $\text{SO}_4^{\bullet-}$ is assumed to add predominantly to C(5), the site of highest electron density,³⁴ when reacting with uracils (**Ia**). In the case of thymines, the steric effect of the C(5)-methyl group seems to make the attack of $\text{SO}_4^{\bullet-}$ to C(6) (**Ib**) likely.¹³

(ii) The Py $\text{SO}_4^{\bullet-}$ adduct decays in times shorter than are observable to form pyrimidine radical cations and SO_4^{2-} (3), while the $\text{Py}^{\bullet+}$ exists in the observable time range as postulated in ref 12. However, this can be ruled out by the observation of $\text{Py}^{\bullet+}$ in nonpolar solution¹⁹ (much higher extinction coefficients in both the lactam and the lactim form; different reactivity) as mentioned above (cf. also Table 2).

(iii) An intermediate and very short-lived $\text{Py}^{\bullet+}$ decays rapidly by deprotonation (6). This mode of decay is most likely in the case of compounds nonmethylated at N(1) yielding radicals of structure **II**. Deprotonation at N(3) seems to be less probable because the intermediate radical cation has nearly no spin³⁵ or charge¹⁰ at N(3) (see Quantum Chemical Calculations). Quantum chemical calculations of the total energies of radicals **II** and **IV** of uracil have demonstrated that deprotonation at N(1) is far more likely than at N(3).¹⁰ For 1-methylthymine, recent FT-EPR studies in our laboratory⁴⁸ resulted in the observation of radical cations in very acidic solution (pH = 1) which were generated by light-induced triplet-sensitized electron transfer (2). Here N(3)-centered radicals seem to exist, but for unusually short times (<1 μs).

(iv) OH-adduct radicals are rapidly formed by the reaction with water if the deprotonation of an intermediate radical cation is impossible due to methylation at N(1). The OH adducts (**IIIa**, **IIIb**) can be formed by hydrolysis of the $\text{SO}_4^{\bullet-}$ adduct ($\text{S}_{\text{N}}2$) or by the nucleophilic addition of H_2O to the radical cation after sulfate elimination ($\text{S}_{\text{N}}1$). The position of the OH group ought

to be determined by the position of the $\text{SO}_4^{\bullet-}$ group in an $\text{S}_{\text{N}}2$ mechanism or the site of the highest positive charge at the radical cation in an $\text{S}_{\text{N}}1$ mechanism.¹³



In the presence of phosphate buffer phosphate ions are additional nucleophiles, that can compete with $\text{H}_2\text{O}/\text{OH}^-$ and lead to the formation of phosphate adducts either in a $\text{S}_{\text{N}}2$ reaction with the sulfate adduct or in a $\text{S}_{\text{N}}1$ reaction with the intermediate radical cation.¹³

Previous quantum chemical calculations¹⁰ of the charge distribution in uracil and 1-methyluracil and their radical cations have proposed that the positive charge of the radical cation mainly resides at C(6) and not C(5). By contrast, our calculations (see below) indicate that the charge of pyrimidine radical cations mainly resides at C(5). This holds for uracil and thymine as well as their derivatives (see Quantum Chemical Calculations). Hence, the formation of C(5)-OH adducts of uracils and of C(6)-OH adducts of thymines cannot be explained by the charge distribution of an intermediate radical cation.

In the case of pyrimidines that are nonmethylated in position 1, two bands are observed at $\lambda \approx 400 \text{ nm}$ and $\lambda \approx 550 \text{ nm}$. Comparing uracil and thymine derivatives, for the thymines the 550 nm absorption is of lower intensity compared to the 400

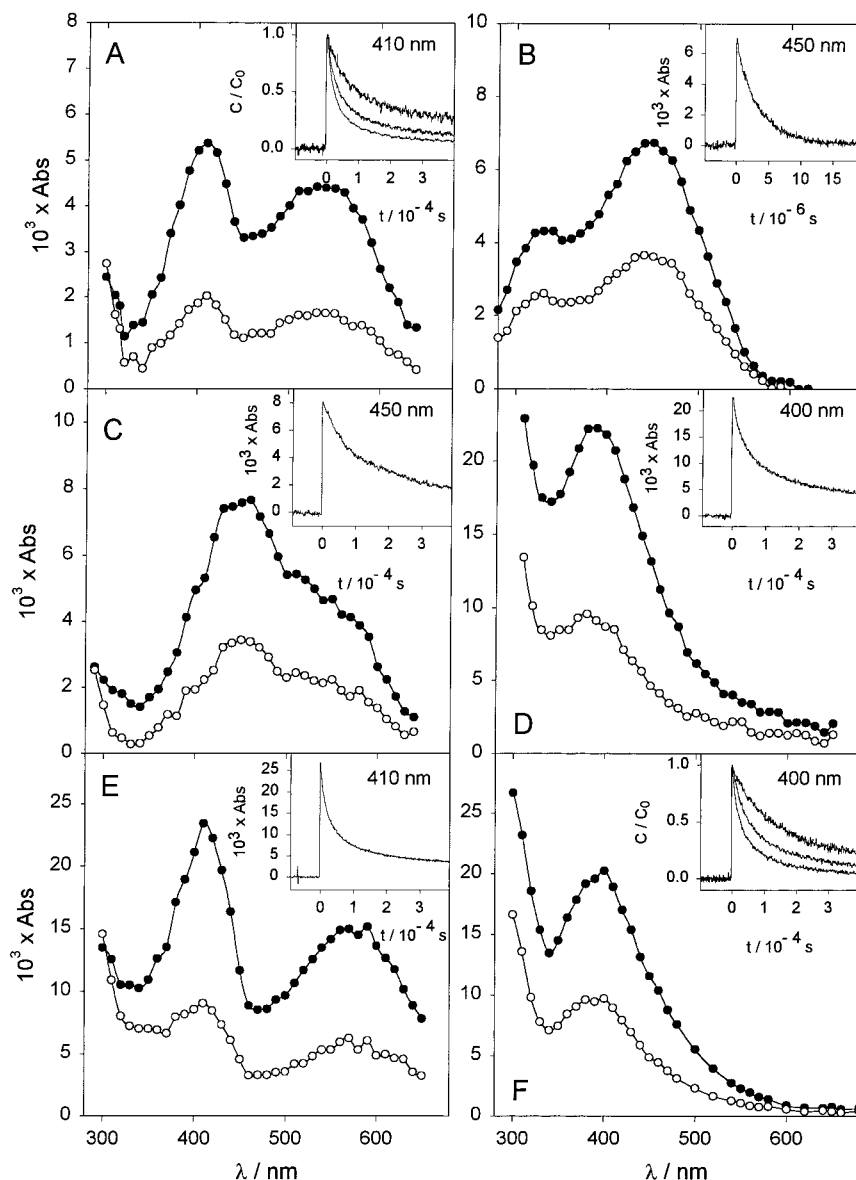


Figure 1. Spectra of $\text{SO}_4^{\bullet-}$ and of transients from the reaction of uracils (5×10^{-3} M) with $\text{SO}_4^{\bullet-}$ at pH 3.5. Nitrogen-saturated solutions containing 0.01 M of $\text{K}_2\text{S}_2\text{O}_8$. Insets: Time-profiles at the absorption maxima. **A:** Uracil (●) 5 μs and (○) 150 μs after the pulse (20 Gy, 0.5 M *tert*-BuOH). Inset: Normalized time profiles after irradiation with pulses of 20, 50, and 100 Gy. **B:** Spectrum of $\text{SO}_4^{\bullet-}$ (●) 500 ns and (○) 2 μs after the pulse of 20 Gy. Solution containing 0.5 M of *tert*-butyl alcohol. **C:** 6-methyluracil (●) 5 μs and (○) 150 μs after the pulse (20 Gy, 0.5 M *tert*-BuOH). **D:** 1-methyluracil (●) 5 μs and (○) 100 μs after the pulse (100 Gy, 2.5 M *tert*-BuOH). **E:** 3-methyluracil (●) 3 μs and (○) 50 μs after the pulse (100 Gy, 2.5 M *tert*-BuOH). **F:** 1,3-dimethyluracil (●) 5 μs and (○) 50 μs after the pulse (100 Gy, 2.5 M *tert*-BuOH). Inset: Normalized time profiles after irradiation with pulses of 20, 50, and 100 Gy.

nm band. Both bands show the same kinetics for decay and also in subsequent scavenger reactions described below. Therefore, it can be concluded that they are caused by the same transient species. ESR and pulse radiolysis studies of the reaction of uracil and thymine with $\text{SO}_4^{\bullet-}$ have identified these species as oxidizing radicals³⁶ with high spin density at N(1) and C(5) (structure **II**).⁷ The same radical is formed in alkaline solution from the reducing C(5)–OH adduct of uracil resulting from the reaction with $\cdot\text{OH}$ radicals.³⁶ In a more recent ESR study, identical radicals were observed after the reaction of excited quinones with uracil, thymine and 6-methylthymine (2).⁵ We assign the transient species derived from 3,6-dimethylthymine as the same radical type (II) due to its similar spectrum (Figure 2C) and reactivity (see below).

The transient spectra of *N*(1)-methylated uracils (1-methyluracil, 1,3-dimethyluracil) show in the vis range only one band peaking at $\lambda \approx 400$ nm (Figure 1D,F). Pulse radiolysis^{9,10} and

ESR^{13,14} studies of the reaction of $\text{SO}_4^{\bullet-}$ with *N*(1)-methylated uracils have shown that the reducing³⁶ C(5)–OH adduct is the main product of this reaction. This holds for low peroxodisulfate concentrations. With higher concentrations of peroxodisulfate (30 mM), a chain reaction with peroxodisulfate^{9,10} selectively oxidizes the reducing C(5)–OH radical and accumulates C(6)–OH radicals, at least on the ms time scale of the ESR experiments.¹³

The transient spectra of *N*(1)-methylated thymines (1-methylthymine, 1,3-dimethylthymine, and 1,3,6-trimethylthymine, cf. Figure 2) appear similar to those of the C(5)–OH radicals, although the transient kinetics differs dramatically. The nitrogen and carbon centered radicals (**II**, **IIIa**) described above decay by a second-order process such as recombination in accordance with reaction 11 depending on the dose per pulse (cf. insets in Figures 1 and 2A,C). The transients derived from the *N*(1)-methylated thymines, however, decay almost irrespective of the

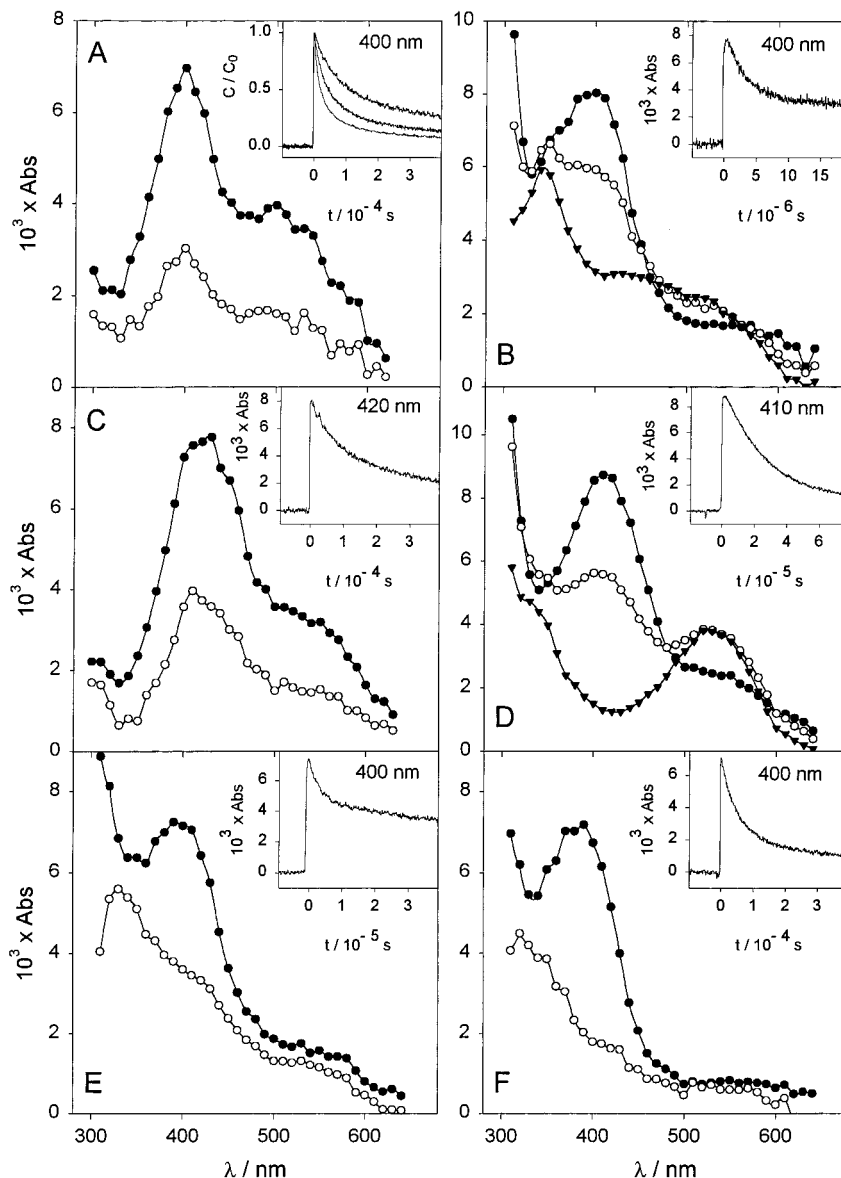
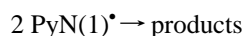
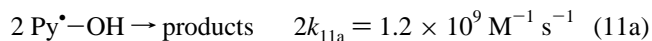


Figure 2. Spectra of transients from the reaction of thymines with $\text{SO}_4^{\bullet-}$. Nitrogen-saturated solutions of thymines (5×10^{-3} M) containing 0.01 M of $\text{K}_2\text{S}_2\text{O}_8$ and 0.5 M of *tert*-butyl alcohol. Pulses of 20 Gy. Insets: Time profiles at the absorption maxima. **A:** Thymine (\bullet) 5 μs and (\circ) 150 μs after the pulse (pH 3.5). Inset: Normalized time profiles after irradiation with pulses of 20, 50, and 100 Gy. **B:** 1,3-dimethylthymine (\bullet) 500 ns, (\circ) 2 μs , and (\blacktriangledown) 15 μs after the pulse (pH 3.5). **C:** 3,6-dimethylthymine (\bullet) 5 μs and (\circ) 150 μs after the pulse (pH 3.5). **D:** 1,3,6-trimethylthymine (\bullet) 2.5 μs , (\circ) 15 μs , and (\blacktriangledown) 75 μs after the pulse (pH 3.5). **E:** 1-methylthymine (\bullet) 1 μs and (\circ) 30 μs after the pulse (pH 2). **F:** 1-methylthymine (\bullet) 5 μs and (\circ) 150 μs after the pulse (pH 7).

dose rate and in much shorter times than the radicals mentioned previously (cf. insets in Figures 2B,D). This is expected for the $\text{SO}_4^{\bullet-}$ adducts (**I**), which ought to decompose in a unimolecular or acid-catalyzed fashion. Therefore, we tentatively assign the transients derived from 1,3-DMT and 1,3,6-TMT to metastable $\text{SO}_4^{\bullet-}$ adducts (**I**) in need of more accurate analysis.

The product spectra resulting from the decay of these primary transient $\text{SO}_4^{\bullet-}$ adducts can be mainly assigned to the C(6)-OH adducts. The product spectrum of 1,3-DMT ($\lambda_{\text{max}} \approx 350$ nm, 450 nm; Figure 2B($-\blacktriangledown-$)) conforms well with the spectrum of the C(6)-OH radical derived from 5-bromo-5,6-dihydro-1,3-dimethyl-6-hydroxythymine by reacting with formate radicals.³⁷ Although similar product spectra were observed with 1,3,6-TMT (Figure 2D($-\blacktriangledown-$)) and 1-MT (Figure 2E,F($-\circ-$)), they seem to be superimposed on absorptions of additional product species below 350 nm and above 500 nm, which we tentatively assign as allyl radicals **V**.



$$2k_{11b} = 1.1\text{--}1.5 \times 10^9 \text{ M}^{-1} \text{ s}^{-1} \quad (11b)$$

1-MT represents a special and even more complicated case. The transient exhibits sensitivity to the pH value in the range around 3. At pH > 3, long-lasting transients are observed which decay by second-order kinetics in the 50 μs scale (inset in Figure 2F), whereas in the strongly acidic system the primary transient decays much faster, i.e., in about 2 μs (inset in Figure 2E), which will be interpreted later on.

Kinetic characterization of $\text{SO}_4^{\bullet-}$ adducts. To find out more about $\text{SO}_4^{\bullet-}$ adducts we reinvestigated the reaction of olefins with $\text{SO}_4^{\bullet-}$ by optical spectroscopy instead of EPR detection as reported by Davies and Gilbert.²⁵ Acrylic acid adds $\text{SO}_4^{\bullet-}$, forming a stable adduct. This adduct was formed in pulse radiolysis at a rate of $k_8 = 6.5 \times 10^7 \text{ M}^{-1} \text{ s}^{-1}$ and shows a UV

TABLE 3. Rate Constants of the Reactions of the Reductants Triphenylamine (TPA), 1,3,5-Trimethoxybenzene (1,3,5-TMB), and 1,4-Dimethoxybenzene (1,4-DMB) with the Radicals Resulting from the Reaction of $\text{SO}_4^{\bullet-}$ with the Pyrimidines

| Py | pH | radical | $k/\text{M}^{-1} \text{s}^{-1}$ | | |
|-----------|-----------|---------|---------------------------------|-------------------|-------------------|
| | | | TPA | 1,3,5-TMB | 1,4-DMB |
| 1,3,6-TMT | 3.5 | I | 1.6×10^9 | 1.3×10^9 | 7.0×10^8 |
| 1,3-DMT | 3.5 | I | | 9.1×10^8 | 1.2×10^9 |
| 1-MT | 1 | I | | 9×10^7 | 1.0×10^9 |
| | 2 | I | | 6.7×10^8 | 1.0×10^9 |
| | 3.5, 5, 7 | I(IIIb) | 3×10^9 | 1.1×10^9 | 1.3×10^9 |
| T | 3.5 | II | 6×10^8 | 8×10^6 | 7.0×10^8 |
| 3,6-DMT | 3.5 | II | 5×10^8 | 8×10^6 | |
| U | 3.5 | II | 1×10^9 | 2.9×10^8 | 1.8×10^9 |
| 3-MU | 3.5 | II | 6×10^8 | 7×10^7 | |
| 6-MU | 3.5 | II | | 9×10^7 | 1.8×10^9 |
| 1-MU | 3.5 | IIIa | <i>a</i> | <i>a</i> | <i>a</i> |
| 1,3-DMU | 3.5 | IIIa | <i>a</i> | <i>a</i> | <i>a</i> |

^a Indicates no reaction with the reductant.

TABLE 4. Rate Constants for the Reactions of Reductants with the Radical Cations of the Pyrimidines Resulting from the Electron Transfer of the Pyrimidines to the Solvent Radical Cations in Acetone and BuCl

| Py | $k/\text{M}^{-1} \text{s}^{-1}$ | | | |
|-----------|---------------------------------|-----------------|----------------------|-----------------|
| | acetone | | BuCl | |
| | TPA | 1,3,5-TMB | TPA | 1,3,5-TMB |
| 1,3,6-TMT | 1.8×10^{10} | 5×10^9 | 1.5×10^{10} | 5×10^9 |
| 3,6-DMT | 1.7×10^{10} | 5×10^9 | <i>a</i> | <i>a</i> |
| 1,3-DMU | 1.9×10^{10} | 5×10^9 | 1×10^{10} | 5×10^9 |
| 1-MU | 1.9×10^{10} | | <i>a</i> | <i>a</i> |

^a Indicates insufficient solubility of Py.

spectrum peaking at 310 nm ($\epsilon = 380 \text{ M}^{-1} \text{ cm}^{-1}$). Like the transients derived from 1,3-DMT and 1,3,6-TMT,¹² it is practically insensitive to oxygen ($k < 5 \times 10^7 \text{ M}^{-1} \text{ s}^{-1}$). Therefore, the latter are not necessarily radical cations.

Similar properties were found for the reaction between allylic alcohol and $\text{SO}_4^{\bullet-}$, i.e., weak product transient absorption with maximum $< 270 \text{ nm}$, but with a higher formation rate of $k_8 = 1.2 \times 10^9 \text{ M}^{-1} \text{ s}^{-1}$.

Oxidation of Additional Scavengers by Py Transients. In a recent paper we checked whether the charge transfer from $\text{Py}^{\bullet+}$ to further scavengers (12a) of lower ionization potential can be used to characterize cationic species.¹⁸ Useful scavengers (reductants, Red) include triphenylamine (TPA) and 1,3,5-trimethoxybenzene (TMB) or 1,4-dimethoxybenzene (DMB), which are described as forming stable radical cations with favorable absorption spectra.^{38,21} The reactions were performed in *n*-butyl chloride or acetone with TPA and TMB, following the reaction sequence (4a or b, 12). Although $\text{Py}^{\bullet+}$ exists in a transient tautomerism with the lactam radical cation predominating in *n*-butyl chloride and the lactime structure in acetone, both forms of $\text{Py}^{\bullet+}$ react in each case with TPA at a diffusion-controlled rate, i.e., $k_{12a}(\text{acetone}) = 2 \times 10^{10} \text{ M}^{-1} \text{ s}^{-1}$ and $k_{12a}(\text{BuCl}) = 1.5 \times 10^{10} \text{ M}^{-1} \text{ s}^{-1}$. The reaction of $\text{Py}^{\bullet+}$ with TMB, however, is in each case slower than diffusion controlled because of the high ionization potential of TMB (Table 4). Figure 3 contains examples of the electron-transfer reaction of $\text{Py}^{\bullet+}$ with TPA. Figure 3A shows transient spectra from the reaction of 1,3,6-TMT^{•+} with TPA in *n*-butyl chloride solution and Figure 3B of 1,3-DMU^{•+} with TPA in acetone. The TPA^{•+} spectra are almost identical in both solvents (inset in Figure 3A). The electron-transfer experiments due to reaction 12a clearly reveal the relation between $\text{Py}^{\bullet+}$ decay and TPA^{•+}

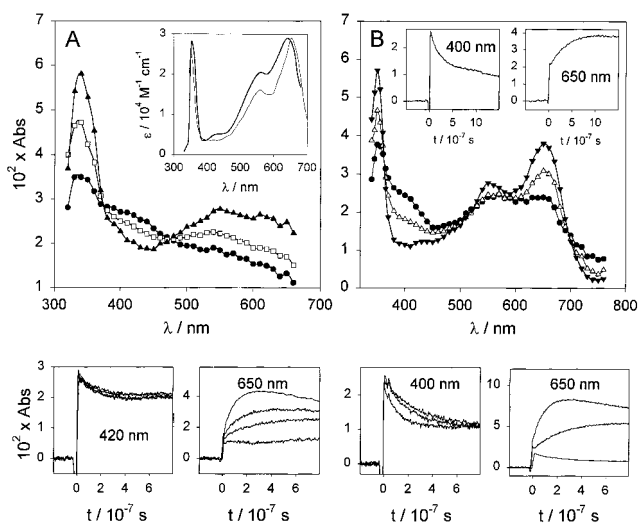
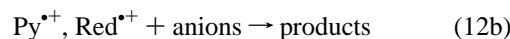


Figure 3. Spectra and time profiles observed during the reaction of pyrimidine radical cations with triphenylamine in nonpolar solvents. Nitrogen saturated solutions irradiated with 150 Gy per pulse. A: Solution of 1,3,6-trimethylthymine (0.01 M) in butyl chloride containing 10^{-4} M of triphenylamine. Spectra (\bullet) 25 ns, (\square) 100 ns, and (\blacktriangle) 750 ns after the pulse. Inset: Spectra of the triphenylamine radical cation in (\rightarrow) butyl chloride and (\leftarrow) acetone. Time profiles: Absorbance changes in the absorption maxima of the 1,3,6-trimethylthymine radical cation (420 nm) and of the triphenylamine radical cation (650 nm) in solutions containing 0, 1, 2, $5 \times 10^{-4} \text{ M}$ of triphenylamine. B: Solution of 1,3-dimethyluracil (0.01 M) in acetone/0.5 M nitromethane containing $5 \times 10^{-5} \text{ M}$ of triphenylamine. Spectra (\bullet) 40 ns, (Δ) 200 ns, and (\blacktriangledown) 1 μs after the pulse. Inset: Absorbance changes in the absorption maxima of the 1,3-dimethyluracil radical cation (400 nm) and of the triphenylamine radical cation (650 nm). Time profiles: Absorbance changes in solutions containing 0, 1, $5 \times 10^{-4} \text{ M}$ of triphenylamine.

formation as demonstrated in Figure 3 for spectral and kinetic behavior.



We decided to use the reactions with the scavengers mentioned to investigate the oxidizing properties of the Py species generated in aqueous solution, especially of the presumed $\text{SO}_4^{\bullet-}$ adducts Deeble et al. assigned to $\text{Py}^{\bullet+}$ and to compare them with the properties of the $\text{Py}^{\bullet+}$ generated in nonpolar solvents.

Among the radical species resulting from the reaction of $\text{SO}_4^{\bullet-}$ with the pyrimidines, the nitrogen radicals II and the C(6)-OH adducts (IIIb) are known to be oxidizing radicals. The latter, however, are not among the transients initially observable. The C(5)-OH adducts (IIIa), on the other hand, are known to be reducing radicals and consistently did not react with the reductants (cf. Table 3). Therefore, the transients responsible for the subsequent oxidation of the reductants are either the nitrogen radical II (13) or the $\text{SO}_4^{\bullet-}$ adduct I (14).

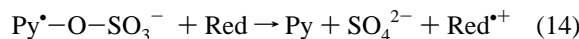
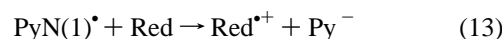


Figure 4 shows the transient spectra and time profiles resulting from the oxidation of Red by the N(1) radical II of uracil (reaction 13) or by the $\text{SO}_4^{\bullet-}$ adduct I of 1,3-dimethylthymine due to eq 14. Figure 4A shows the decay of the adduct I (400 nm) and the corresponding formation of TMB^{•+} (480 nm), clearly separated in spectra and kinetics. The decay of the N(1)

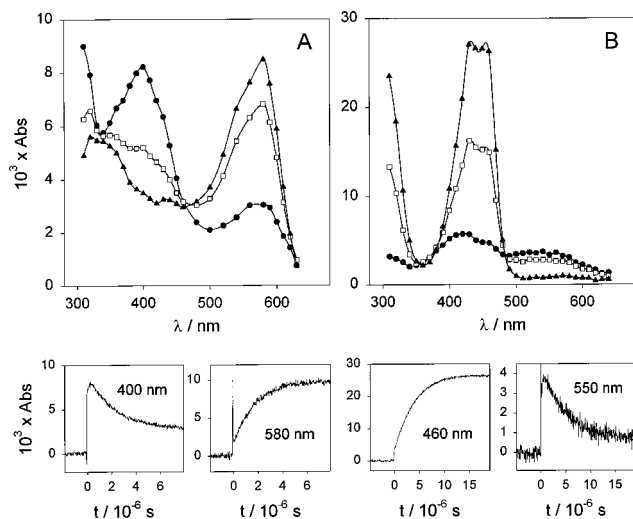


Figure 4. Spectra and time profiles observed during the reaction of pyrimidine transients with methoxybenzenes in aqueous solution after irradiation with pulses of 20 Gy. Pyrimidine transients resulting from the reaction with $\text{SO}_4^{\cdot-}$ in nitrogen saturated solutions of the pyrimidines (5×10^{-3} M) containing 0.01 M of $\text{K}_2\text{S}_2\text{O}_8$ and 0.5 M of *tert*-butanol. **A:** Solution of 1,3-dimethylthymine containing 10^{-4} M of 1,3,5-trimethoxybenzene. Spectra (●) 500 ns, (□) 2 μs , and (▲) 5 μs after the pulse. Time profiles: Absorbance changes in the absorption maxima of the 1,3-dimethylthymine transient (400 nm) and of the 1,3,5-trimethoxybenzene radical cation (580 nm). **B:** Solution of uracil containing 10^{-4} M of 1,4-dimethoxybenzene. Spectra (●) 500 ns, (□) 2.5 μs , and (▲) 15 μs after the pulse. Time profiles: Absorbance changes in the absorption maxima of the uracil transient (550 nm) and of the 1,4-dimethoxybenzene radical cation (460 nm).

radical **II** and the formation of $\text{DMB}^{\cdot+}$ are depicted in Figure 4B. Because of the blue-shifted spectrum of $\text{DMB}^{\cdot+}$ (460 nm), in this case the decay reaction was analyzed at 550 nm.

Bimolecular rate constants were determined from the time profiles of the Py species decay and of $\text{Red}^{\cdot+}$ formation by plotting the pseudo-first-order rate constants vs the concentration of Red, and also by modeling the time profiles with the proposed mechanism using the software ACCUCHEM.³⁹

For the examples shown in Figure 4, the rate constants amount to $k_{14} = 9 \times 10^8 \text{ M}^{-1} \text{ s}^{-1}$ and $k_{13} = 2 \times 10^9 \text{ M}^{-1} \text{ s}^{-1}$, i.e., comparably high values. Similarly high rate constants were found for the other pyrimidine transients of type **I**, whereas for **II** the values differ considerably between uracil and thymine derivatives. The rate constants for the reactions of the reductants with transients derived from various pyrimidines in aqueous solution are listed in Table 3. Those determined for the reaction of $\text{Py}^{\cdot+}$ in acetone or in *n*-butyl chloride are given in Table 4. The oxidation reactions 13 and 14 are surprisingly rapid but do not reach the diffusion-controlled limit (as attained in the radical cation reaction with TPA in nonpolar solvents), that in water amounts to about $6 \times 10^9 \text{ M}^{-1} \text{ s}^{-1}$.

Taking into account the different viscosities as well, the reactions performed in water do not reach the diffusion-controlled limit with TPA and display a slightly slower and, therefore, more activation-controlled reaction with TMB. Because reactions of the radicals of the type **I** and **II** are not free electron transfer reactions in the narrow sense, their rate constants strongly depend on the reduction potential differences between radical and reductant. The one-electron oxidation potentials of the reductants are 1.29,⁴⁰ 1.58,⁴¹ and 1.67 V⁴² (NHE) for TPA, DMB, and TMB, respectively, and qualitatively explain the different rate constants of the reaction between oxidizing pyrimidine radicals and different reductants. Reduction potentials of radicals derived from different pyrimidines exist¹⁶

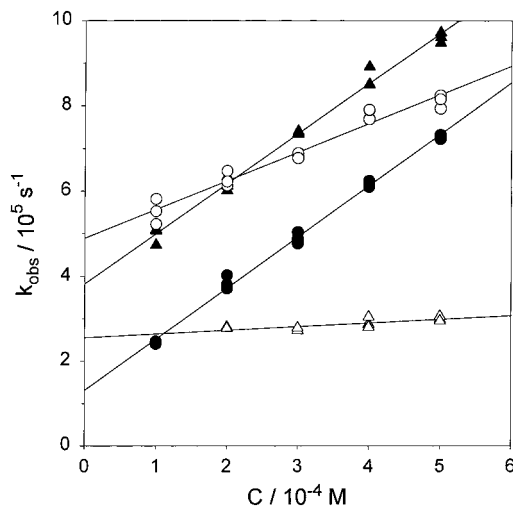
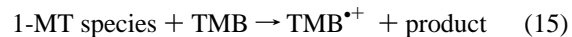


Figure 5. Observed pseudo-first-order rate constants k_{obs} of the formation of 1,3,5-trimethoxybenzene radical cations from the reaction with transients of 1-methylthymine at various pH values as a function of the 1,3,5-trimethoxybenzene concentration. Values of k_{obs} were obtained from exponential fits of the absorbance change observed at 580 nm in nitrogen saturated solutions of 1-methylthymine (5×10^{-3} M) containing 0.01 M of $\text{K}_2\text{S}_2\text{O}_8$, 0.5 M of *tert*-butanol and $(1-5) \times 10^{-4}$ M of 1,3,5-trimethoxybenzene after pulses of 20 Gy. Solutions at pH 7 (●), 3.5 (▲), and 2 (○) with 20 mM of phosphate buffer. At pH 1 (△) with sulfuric acid.

but do not seem to be sufficiently reliable.⁴³ For the reactions in the organic solvents, gas-phase ionization potentials are a more appropriate parameter to explain the different rate constants observed with TPA and TMB. The ionization potentials of uracil and thymine are 9.59⁴⁴ and 9.18 eV,⁴⁴ while those of the higher methylated derivatives can be estimated to be 8–9 eV.⁴⁵ The ionization potentials of TPA and TMB amount to 7.00⁴⁶ and 8.11 eV,⁴⁷ which explains the diffusion-controlled reaction of TPA and the activation-controlled reaction of TMB with the pyrimidine radical cations.

To sum up, the rate constants of the electron-transfer reactions facilitate the classification of the reaction path in accordance with either reaction 12a (cationic, driven by $\text{Py}^{\cdot+}$), reaction 14 ($\text{SO}_4^{\cdot-}$ adduct caused), or reaction 13 (N(1)-radical caused). This analysis confirms the assignment of the transients in accordance with the numbers given in the third column of Table 3.

1-Methylthymine as a Special Case. A complex kinetic behavior was observed for 1-MT as already found by Deeb et al.¹² Very different from 1-MU which forms as an observable product the C(5)-OH adduct **III**, 1-MT exhibits pH-dependent behavior and at pH > 3 long-lasting species decaying at a normal bimolecular rate of $2k \approx 10^9 \text{ M}^{-1} \text{ s}^{-1}$ as observed for the Py radicals **II** and **IIIa**. At pH < 3, its lifetime is 10 times shorter and the species decays within a few microseconds, i.e., in a transient concentration-independent manner. Concomitant with its decrease in lifetime, a marked reactivity change in the reaction with the reductant TMB is observed. The k_{15} value drops from $10^9 \text{ M}^{-1} \text{ s}^{-1}$ at pH = 3 (as typical for **I**) to less than $10^8 \text{ M}^{-1} \text{ s}^{-1}$ at pH = 1 (see Table 3).



Plots of the pseudo-first-order rate constants $k_{15}(\text{obs})$ versus the concentration of TMB (Figure 5) yield the rate constants given in Table 3. The extrapolated intercept on the abscissa gives the total rate of all reactions competing with (15) such as recombination or, as is more likely here, first-order decay of the reactive 1-MT species in the absence of the reductant (cf. Figure 5).

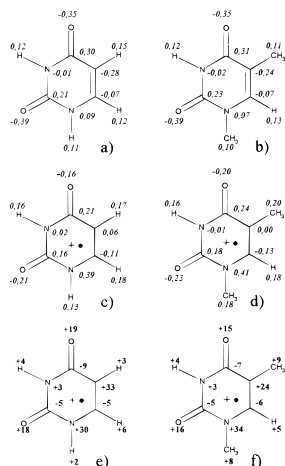
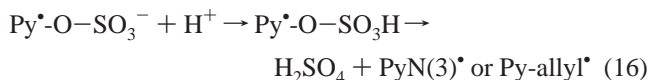


Figure 6. Calculated atomic charges of uracil and 1-methylthymine (a, b) and their radical cations (c, d). The changes of atomic charges upon ionization are given (in percent) with structures (e) and (f).

When analyzing this intercept in comparison to the transient time profiles monitoring the decay of the 1-MT species, a very surprising picture emerged. At low pH the inverse of the intercepts, i.e., the transient lifetimes of 2–3 μs , conform with those taken from the time profiles. At pH > 3 the inverse of the intercept increases with pH to a value of about 7 μs at pH 7. However, the transient half-life taken from the time profiles of the 1-MT species amounts to about 50 μs ($2k_{11a} = 2.8 \times 10^9 \text{ M}^{-1} \text{ s}^{-1}$) at pH 7. Therefore, we conclude that two transients exhibit practically the same absorption spectrum but different kinetics. We tentatively assign the transient reacting rapidly with the reductant (reaction 15) to the $\text{SO}_4^{\bullet-}$ adduct **I** of 1-MT because k_{15} amounts to similar values as also observed for the adducts of 1,3-DMT and 1,3,6-TMT, i.e., $10^9 \text{ M}^{-1} \text{ s}^{-1}$. In very acidic solution this transient may protolyse with the formation of a less reactive radical. This product radical might be the N(3) radical (structure **IV**) or more probably the allyl radical (structure **V**), although it cannot be decided which from our experimental material.



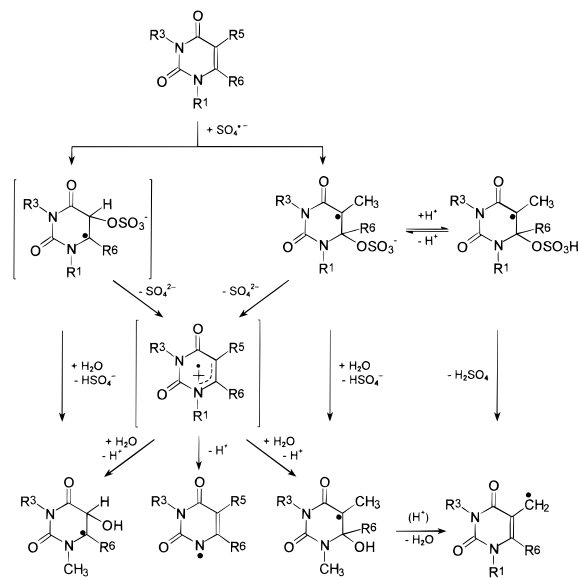
At pH values higher than 3 the adduct decays by hydrolysis to form the C(6)-OH adduct (**IIIb**) (see Figure 2E, F). Although the C(6)-OH adduct ought to be an oxidizing radical, it does not markedly contribute to the oxidation of TMB (reaction 15), otherwise the intercept of the pseudo-first-order plot (Figure 5, pH 7) would be considerably smaller.

Here we deviate from the mechanistic interpretation of Deeble et al.,¹² which assigned the species observed to $\text{Py}^{\bullet+}$. With the benefit of information about the reactions of the Py transients with the reductants (12–15), it can be shown that these effects must be interpreted in terms of metastable $\text{SO}_4^{\bullet-}$ adducts rather than radical cations.

Quantum Chemical Calculations. PM3/SCI-calculated vertical excitation energies of C(6)- SO_4 -adducts derived from 1-methylthymine, 1,3-dimethylthymine, and 1,3,6-trimethylthymine amount to 390–410 nm, which tallies well with the absorptions assigned to the sulfate adducts.

Atomic charges were calculated for the whole set of methylated pyrimidines and their radical cations. Figure 6 lists the atomic charges of uracil, 1-methylthymine and their radical cations together with the charge differences between the neutral molecules and their radical cations.

SCHEME 1: Transformations of the Sulfate Adducts Resulting from the Reaction of Pyrimidines with $\text{SO}_4^{\bullet-}$.



These calculations give a reasonable description of the positively charged centers at C(5) and N(1) which are favored for nucleophilic attack.

Mechanism of the Oxidation of Py by $\text{SO}_4^{\bullet-}$: The electron transfer (4) in nonpolar solution from Py to the parent solvent radical cations yields Py radical cations as observable species which exist for a few hundred nanoseconds and decay by neutralization with the counterion. It is from these experiments that the pronounced kinetic and spectral properties, especially the markedly high extinction coefficients, are known.

The reaction of the pyrimidines with sulfate radical anions in aqueous solution proceeds via a metastable adduct $\text{Py}^{\bullet}\text{-SO}_4^-$, which decays by hydrolysis or protolysis to form N and C centered radicals (**II**, **III**) depending on the methylation pattern of the pyrimidines. There is no direct experimental evidence of an intermediate Py radical cation. However, if $\text{Py}^{\bullet+}$ were passed as an intermediate of solvolysis, its lifetime would be shorter than the experimental time resolution of a few nanoseconds. This situation is formulated in the reaction scheme.

Depending on the methylation pattern, the N(1) radical **II** or the C(5) OH-adduct **IIIa** appear as primary observable transients for uracils and thymines (left part of the diagram). The former could be best explained as being formed via an intermediate $\text{Py}^{\bullet+}$ and its immediate deprotonation. For the formation of **IIIa** both channels $\text{S}_{\text{N}}1$ and $\text{S}_{\text{N}}2$ could be considered.

In the cases of 1,3-DMT and 1,3,6-TMT, the adducts $\text{Py}^{\bullet}\text{-SO}_4^-$ could be directly observed and were characterized as strongly oxidizing species. Although more complicated, this fact also holds for 1-MT. The 1-MT adduct **Ib** hydrolyses at medium pH values, forming C-centered radicals of type **IIIb**, and protolyses under very acidic conditions (pH < 3) to form a radical product of postulated allyl radical structure **V**. The decay of the directly observed $\text{SO}_4^{\bullet-}$ adducts **I** mainly yields the C(6) OH-adduct **IIIb** and possibly also the allyl radical **V**. The $\text{Py}^{\bullet+}$ exists (if at all) for less than 20 ns. The fact that solely the C(6) adduct **IIIb** of the OH-adducts is observed makes the $\text{S}_{\text{N}}1$ path less probable because C(5) ought to be the preferred site of a nucleophilic attack on the radical cation. Therefore, we favor the $\text{S}_{\text{N}}2$ channel of solvolysis.

The intermediate radical transients of Py and the adducts $\text{Py}^{\bullet}\text{-SO}_4^-$ were characterized by subsequent oxidation reactions

involving TPA, 1,4-DMB, and 1,3,5-TMB, except for the radicals of structure **IIIa** that do not oxidize.

References and Notes

- (1) von Sonntag, C. *The Chemical Basis of Radiation Biology*; Taylor and Francis: London, 1987. Hüttermann, J.; Köhnlein, W.; Téoule, R.; Bertinchamps, A. J. Eds.; *Effects of Ionizing Radiation on DNA*; Springer: Berlin, 1978.
- (2) von Sonntag, C.; Schuchmann, H.-P. *Int. J. Radiat. Biol.* **1986**, *49*, 1. Bernhard, W. A. *Adv. Radiat. Biol.* **1981**, *9*, 199. Steenken, S. *Biol. Chem.* **1997**, *378*, 1293.
- (3) Lemaire, D. G. E.; Bothe, E.; Schulte-Frohlinde, D. *Int. J. Radiat. Biol.* **1984**, *45*, 351. Schulte-Frohlinde, D.; Opitz, J.; Görner, H.; Bothe, E. *Int. J. Radiat. Biol.* **1985**, *48*, 397. Catterall, H.; Davies, M. J.; Gilbert, B. C. *J. Chem. Soc., Perkin Trans 2* **1992**, 1379.
- (4) Görner, H. J. *Photochem. Photobiol., B* **1994**, *26*, 117 and references therein.
- (5) Geimer, J.; Brede, O.; Beckert, D. *Chem. Phys. Lett.* **1997**, *276*, 411.
- (6) Wood, P. D.; Redmond, R. W. *J. Am. Chem. Soc.* **1996**, *118*, 4256.
- (7) Bansal, K. M.; Fessenden, R. W. *Radiat. Res.* **1978**, *75*, 497.
- (8) Fujita, S.; Nagata, Y. *Radiat. Res.* **1988**, *114*, 7.
- (9) von Sonntag, C.; Rashid, R.; Schuchmann, H.-P.; Mark, F. *Free Radical Res. Commun.* **1989**, *6*, 111.
- (10) Schuchmann, H.-P.; Deeble, D. J.; Olbrich, G.; von Sonntag, C. *Int. J. Radiat. Biol.* **1987**, *51*, 441.
- (11) Bothe, E.; Deeble, D. J.; Lemaire, D. G. E.; Rashid, R.; Schuchmann, M. N.; Schuchmann, H.-P.; Schulte-Frohlinde, D.; Steenken, S.; von Sonntag, C. *Radiat. Phys. Chem.* **1990**, *36*, 149.
- (12) Deeble, D. J.; Schuchmann, M. N.; Steenken, S.; von Sonntag, C. *J. Phys. Chem.* **1990**, *94*, 8186.
- (13) Behrens, G.; Hildenbrand, K.; Schulte-Frohlinde, D.; Herak, J. N. *J. Chem. Soc., Perkin Trans. 2* **1988**, 305.
- (14) Hildenbrand, K. *J. Chem. Soc., Perkin Trans. 2* **1995**, 2153.
- (15) Novais, H. M.; Steenken, S. *J. Phys. Chem.* **1987**, *91*, 426.
- (16) Jovanovic, S. V.; Simic, M. G. *J. Phys. Chem.* **1986**, *90*, 974.
- (17) Mehnert, R.; Brede, O.; Naumann, W. *Ber. Bunsen-Ges. Phys. Chem.* **1982**, *86*, 525. Brede, O.; Mehnert, R.; Naumann, W. *Chem. Phys.* **1987**, *115*, 279.
- (18) Lomoth, R.; Brede, O. *Chem. Phys. Lett.* **1998**, *288*, 47.
- (19) Lomoth, R.; Brede, O.; Naumov, S. *J. Phys. Chem. A* **1999** *103*, 2641.
- (20) Neta, P.; Madhavan, V.; Zemel, H.; Fessenden, R. W. *J. Am. Chem. Soc.*, **1977**, *99*, 163.
- (21) O'Neill, P.; Steenken, S.; Schulte-Frohlinde, D. *J. Phys. Chem.* **1975**, *79*, 2773.
- (22) O'Neill, P.; Steenken, S.; Schulte-Frohlinde, D. *J. Phys. Chem.* **1977**, *81*, 26.
- (23) Sehested, K.; Holcman, C.; Hart, E. J. *J. Phys. Chem.* **1977**, *81*, 1363.
- (24) Norman, R. O. C.; Storey, P. M.; West, P. R. *J. Chem. Soc. B* **1970**, 1087.
- (25) Davies, M. J.; Gilbert, B. C. *J. Chem. Soc., Perkin. Trans. 2* **1984**, 1809.
- (26) Brown, D. J., Mason, S. F., Eds., *The Pyrimidines*; Wiley Interscience Publishers: New York, 1962.
- (27) Stewart, J. P. P. *J. Comput. Chem.* **1989**, *209*, 221; *J. Comput.-Aided Mol. Design* **1990**, *4*, 1.
- (28) Faria, J. L.; Steenken S. *J. Phys. Chem.* **1992**, *96*, 10869.
- (29) Roebke, W.; Renz, M.; Henglein, A. *Int. J. Radiat. Phys. Chem.* **1969**, *1*, 39.
- (30) Balkas, T. I.; Fendler, J. H.; Schuler, R. H. *J. Phys. Chem.* **1970**, *74*, 4497.
- (31) Buxton, G. V.; Greenstock, C. L.; Helman, W. P.; Ross, A. B. *J. Phys. Chem. Ref. Data* **1988**, *17*, 513.
- (32) Eibenberger, H.; Steenken, S.; O'Neill, P.; Schulte-Frohlinde, D. *J. Phys. Chem.* **1978**, *82*, 749. Clifton, C. L.; Huie, R. E. *Int. J. Chem. Kinet.* **1989**, *21*, 677.
- (33) Hayon, E.; Treinin, A.; Wilf, J. *J. Am. Chem. Soc.* **1972**, *94*, 47.
- (34) Pullman, B.; Pullman, A. *Quantum Biochemistry*; Wiley: New York, 1963; p 225.
- (35) Oloff, H.; Hüttermann, J. *J. Magn. Reson.* **1980**, *40*, 415.
- (36) Fujita, S.; Steenken S. *J. Am. Chem. Soc.* **1981**, *103*, 2540.
- (37) Deeble, D. J.; von Sonntag, C. *Z. Naturforsch.* **1985**, *40c*, 925.
- (38) Shida, T. *Electronic Absorption Spectra of Radical Ions*; Elsevier: Amsterdam, 1988. Burrows, H. D.; Greatorex, D.; Kemp, J. *J. Phys. Chem.* **1972**, *76*, 20. Shoute, L. C. T.; Neta, P. *J. Phys. Chem.* **1990**, *94*, 2447.
- (39) Braun, W.; Herron, J. T.; Kahaner, D. Computer Program for Modelling Complex Reaction Systems; National Bureau of Standards: Gaithersburg.
- (40) Chen, C. H.; Brighty, K. E.; Michaels, F. M. *J. Org. Chem.* **1981**, *46*, 361.
- (41) Mattes, S. L.; Farid, S. *J. Am. Chem. Soc.* **1982**, *104*, 1454.
- (42) Balardini, R.; Varani, G.; Indelli, T.; Scandola, F.; Balzani, V. *J. Am. Chem. Soc.* **1978**, *100*, 7219.
- (43) Seidel, C. A. M.; Schulz, A.; Sauer, M. H. M. *J. Phys. Chem.* **1996**, *100*, 5541.
- (44) Urano, S.; Yang, X.; LeBreton, P. R. *J. Mol. Struct.* **1989**, *214*, 315.
- (45) S. Steenken. Private communication.
- (46) Murov, S. L.; Carmichael, I.; Hug, G. L. *Handbook of Photochemistry*, 2nd ed.; Marcel Dekker: New York, 1993.
- (47) Yagci, Y.; Schnabel, W.; Wilpert, A.; Bending, J., *J. Chem. Soc., Faraday Trans. 2* **1994**, *90*, 287.
- (48) Beckert, D.; Geimer, J. *J. Phys. Chem. A* **1999**, *103*, 3991.